GEOMICROBIOLOGY JOURNAL
2025, VOL. 42, NO. 5, 390–405
https://doi.org/10.1080/01490451.2025.2467417

Subfossil Fracture-Related Euendolithic Micro-burrows in Marble and Limestone

Cees W. Passchier[a], Trudy M. Wassenaar[b], Nora Groschopf[a], Anne Jantschke[a], and Regina Mertz-Kraus[a]

[a]Department of Earth Sciences, Johannes Gutenberg University, Mainz, Germany; [b]Molecular Microbiology and Genomics Consultants, Zotzenheim, Germany

ABSTRACT

Marble and limestone in desert environments of Namibia, Oman and Saudi Arabia is found to be affected by micro-burrows formed by inferred endolithic microbiological activity. Up to 10 m long bands of parallel micro-burrows, as wide as 0.5 mm and up to 30 mm long, formed along fractures inside the rock. The structures are exposed by erosion and appear to be subfossil and no longer active. In some cases, the micro-burrows are bordered by calcrete that formed along fractures. In fresh outcrops, the micro-burrows are filled with white calcium carbonate with internal structures and depleted in several elements. The rims of the micro-burrows contain 1 µm wide contours enriched in P and S. Fluorescence microscopy, Raman spectroscopy and $\delta^{13}C$ values confirm the presence of biological material. The fossils are too old to conserve DNA or protein. It is presently unclear which organism may have been responsible for the formation of these structures, that are described here for the first time.

ARTICLE HISTORY
Received 20 July 2024
Accepted 11 February 2025

KEYWORDS
Limestone; marble; calcrete; endolith; desert; erosion

Introduction

The global carbon cycle describes how carbon atoms are exchanged between the Earth's atmosphere (gaseous CO_2) and the main global carbon sinks: the oceans (where dissolved CO_2 results in bicarbonate ions), terrestrial carbonate deposits, and living and fossilized biomatter (Prentice et al. 2001). Most global carbon is present as carbonate rocks, such as limestone and marble. It is therefore important to understand how terrestrial organisms can affect carbon stored in carbonate rocks, and on which scale this happens. For that purpose, all organisms that constitute the biosphere affecting carbonate rocks must be incorporated into any considerations and calculations that estimate carbon cycle magnitudes.

Microorganisms can immobilize carbon into carbon sinks by the formation of calcite. This microbial deposition is mainly driven by marine processes (Tanhua et al. 2013) but occurs on land on a smaller scale as well. The term endostromatolites is used to describe fissure calcrete of biological origin that formed in extreme terrestrial environments such as the Arctic and other periglacial regions (Clark et al. 2004; Lacelle et al. 2009). However, microorganisms may also assist in local removal or reworking of calcite, living on the surface or inside the fabric of rocky outcrops or boulders. Such endolithic microorganisms can occur in several habitats of rock surfaces and are divided into cryptoendoliths that inhabit crypts in the rock, chasmoendoliths that colonize fissures, hypoendoliths that occupy cavities at the bottom of boulders, and euendoliths that actively bore into rocks, especially into carbonates (Dievart et al. 2022; Golubic et al. 1981; Wierzchos et al. 2018). Endolithic microorganisms may create their own niche by removal of rock material (most often calcite) and typically survive in extreme environments. For instance, as recently reviewed (Wierzchos et al. 2018), cyanobacteria and other endoliths colonize rocks in the hyperarid Atacama Desert (Chile). The contribution of carbon release by such biological activity toward the global carbon cycle is most likely negligible, though hard to determine. Where biological activity assists in weathering of terrestrial carbonate rocks on a larger scale, that contribution may be significant, especially in desert environments that cover large parts of the Earth, occurring in places where such activity may not be expected.

In this paper, we describe marbles and limestones from Namibia, Oman and Saudi Arabia that have been eroded and replaced by an agent, forming bands of micro-burrows. Since no abiogenic mechanisms can explain the generation of these structures, we infer that they must be a result of biological activity. The product of this activity is observed on a relatively large scale in outcrops of these carbonate rocks, which are at present located in a hyperarid climate. The aim of this paper is to draw attention to the presence of these structures in southern Africa and the Arabian Peninsula, to present a description and to summarize what is presently known about these

CONTACT Cees W. Passchier cpasschi@uni-mainz.de Department of Earth Sciences, Johannes Gutenberg University, 55128 Mainz, Germany.
Supplemental data for this article can be accessed online at https://doi.org/10.1080/01490451.2025.2467417.

structures. We hope to inspire field workers and specialists in the study of endoliths to determine if similar structures can be found in other continents and environments, and to establish which microorganisms might be responsible for their formation. It will then be interesting to see if these still exist or are extinct, and to determine their role in the global carbon cycle.

Material and methods

Locations of the field observations

Field observations presented here are mainly from Namibia. The coordinates of the best examples, used in this paper, were: 28.34562 S, 16.76303 E; 20.48690 S, 14.33225 E; 20.51489 S, 14.37188 E and 20.83226 S, 14.12512 E. The local geology is characterized by the presence of two older Proterozoic cratons, the Angola and Kalahari cratons, separated by a belt of strongly deformed marine sediments of Neoproterozoic age, which were deformed and metamorphosed in the Cambrian (Frimmel and Miller 2009; Miller 1983; Porada 1979; Prave and Hoffmann 1995). The marbles consist of banded coarse-crystalline $CaCO_3$ with traces of Si, Mg, Fe, Al, Sr, Mn, and other elements. The composition of the marbles is still comparable to marine limestone. The marble layers are folded, causing variable *in situ* orientation of the layering. After the Cambrian deformation and metamorphism, the rocks were long buried and covered by Mesozoic sediments, but surfaced in the Tertiary and weathered to their recent outcrop geometry. Calcrete of probably Neogene—Pleistocene age (Pickford 2000) formed on top of the marbles and in fractures.

The coastal strip in Namibia is extremely arid (Heine 1998), but wetter periods associated with calcrete formation have occurred in the past, the last being 16,000–13,000 years before present (Shaw and Thomas 1996). The significant weathering of the structures and associated calcrete described here, however, suggest that these must be older, probably between 1 and 3 My (Heine 1998; Pickford 2000).

Observations and samples collected in Oman were from the southern flank of the Jebel Akhdar anticlines around 23.17102 N, 57.27191 E. Furthermore, observations were made at two locations with colored marbles in Saudi Arabia, at Wadi Ad Dawasir and Ad Duwadimi, Riyadh Region (20.77737 N, 43.94699 E; 24.34384 N, 3.72993 E).

Microscopy

Petrographic thin sections were produced at 30 and 100 µm thickness. Microscopy was performed with a LEICA petrographic microscope (Leitz DMRD). Thin sections of 30 µm were investigated under plain- and cross-polarized light, and 100 µm thin sections were photographed in reflected and in transmitted light and used for analyses.

Laser ablation-Inductively coupled plasma mass spectrometry (LA-ICP-MS)

Trace element analyses were performed by LA-ICP-MS using an ArF Excimer laser system (ESI NWR193, TwoVol2 ablation cell) with an output wavelength of 193 nm coupled to an Agilent 7500ce ICP-MS. Reference material is described elsewhere (Jochum et al. 2005, 2011). Analyses were carried out on polished 100 µm thin sections, creating lines of spots with a spot size of 100 or 50 µm and a spacing of 100 µm using a repetition rate of 10 Hz and an energy density of approximately 3.0 J/cm^2. For further details see Supplementary file.

Electron microprobe analysis (EMPA)

Element compositions of thin-section surfaces were determined by Wavelength-Dispersive Spectroscopy (WDS) with a JEOL JXA-8200 electron microprobe (JEOL, Eching, Germany). The conditions were 15 kV accelerating voltage, 8 nA beam current with a beam diameter set to 5 µm. Peak counting times were 20 s for major elements, 30–40 s for minor elements and 60 s for S and P. Sets of reference materials with well characterized natural and synthetic oxides and minerals (P&H Development Ltd., Whitby, England and Astimex Scientific Ltd., Toronto, Canada) were used for calibration. The routine ZAF procedure (correcting for atomic effects Z, absorption A and fluorescence F) in the JEOL software was used for data processing. The applied conditions for X-ray element maps of Mg, Al, Si, P, and S (including backscattered images) were 15 kV, 30 nA with a resolution of 0.5–2 µm/pixel and a dwell time of 280 ms/pixel.

Fluorescence microscopy

Epifluorescence microscopy was carried out using an Olympus IX70 inverted microscope with a UPLANF 4x (NA 0.13) and CPLANFL 10x (NA 0.3) objective. Thin section fluorescence was excited with a UV-mercury lamp (100 W, Olympus U-RFL-T) and observed with a U-MNU2 excitation filter (Olympus, BP 360–370 excitation, DM 400 dichromatic mirror, 420LP emission filter). Images were taken with a Canon EOS 550D camera and processed using ImageJ.

Raman analysis

Raman maps were collected on 30 µm thin sections using a Horiba Yobin Yvon LabRam 800 (Horiba Scientific), a confocal Raman high-resolution spectrometer equipped with a Si-based CCD detector (Peltier-cooled). The system is based on an integrated BX41 upright optical microscope (Olympus) and an automated x–y stage.

Samples were measured with a 50× long-distance objective (Leica PL FLUOTAR L 50x/NA 0.55) using 532 nm laser excitation. The analyzed areas showed fluorescence, therefore, laser power was reduced to 25% (approximately 5.25 mW) and a delay time of 180 s was used for quenching. All spectra were collected in the range of 100–3250 cm^{-1} using a 300 gr/mm grating, a slit width of 100 µm, and a hole diameter of 400 µm. The spectrometer was calibrated using the 520.7 cm^{-1} band of silicon.

A Raman map (145 × 93 µm^2) was collected with 5 µm step size, 1 s exposure time and 10 accumulations.

Spectral datasets were imported into the SpectralImaging software based on Matlab provided and developed by Matthias Finger (spectralimaging@outlook.com). First, spectra were cut (1820–100 cm^{-1}) and baseline corrected by asymmetric least squares correction (smoothness 2.5, asymmetry 2). Spectra were smoothed using the Savitzky-Golay algorithm (2nd degree over 11 datapoints) before multivariate analysis. Non-negative Matrix Factorization was then used to identify and visualize individual principal components.

Stable isotope analysis

Two samples from Namibia (designated 'Na-2' and 'Na-N') were sampled using a microdrill for stable oxygen and carbon isotope analysis. The white filling of the micro-burrows was carefully extracted and isolated. In addition, the surrounding modified carbonate, two layer types of the host marble, and calcrete present in the fracture from which the micro-burrows branched into the marble, were sampled with a larger size drill. All isolated powders were analyzed for stable isotopes at the University of Innsbruck using a semi-automated device (Gasbench II) linked to a ThermoFisher Delta V Plus isotope ratio mass spectrometer. Isotope values are reported on the Vienna Peedee Belemnite (VPDB) scale. By experience, long-term precision exceeds 0.1‰, for both $\delta^{13}C$ and $\delta^{18}O$ (Spötl and Vennemann 2003).

Terminology used

A graphical description of the terminology used is given in Figure S1. The main features described here are named 'micro-burrows', with 'micro-burrow bands' specifying a collection of parallel narrow tubes that are mostly evenly spaced in the rock. The micro-burrows can be void or filled with white material. Their edges are called straight if all micro-burrows are aligned at one edge, or ragged if their length differs. Other terminology is summarized in Figure S1.

Results

Field and macroscopic observations

The extensive outcrops of Neoproterozoic marble in the desert of western Namibia commonly show the presence of groups of micro-burrows at various locations between 10 and 150 km from the coast between 20 and 29°S (Figure 1A). Sites where they are easily found are near Twijfelfontein and along the Ugab and Huab rivers. Micro-burrows are present as groups of narrow, parallel borings in the rock that occur in bands, which we call micro-burrow bands. A single band (Figure 1B) illustrates how this differs from the typical irregular karst erosion. Multiple micro-burrow bands in the outcrop of Figure 1(C) have undergone various degrees of erosion. Alternating blue, grey and white layers in the marble, caused by minor differences in composition, are still visible in the remaining micro-burrow walls, suggesting that they formed by removal of original rock material. In fresh outcrops with rock on both edges of a micro-burrow band (see Figure S1 for descriptive terminology), the micro-burrows are loosely filled with white micritic calcite which is commonly in stark contrast with the darker host rock. The upper edge of micro-burrow bands to the original rock is quite sharp and straight, while the lower edge is more often irregular or ragged, since micro-burrows can penetrate with variable lengths, to up to 30 mm for 0.5 mm wide micro-burrows. All individual micro-burrows are strictly parallel, and never cross or diverge. A thin white micritic band is commonly visible along the straight edge, as in Figure 2(A). Commonly, calcrete is also present at their straight edge (Figure 2B,C), again often separated by a thin white layer. The micro-burrow bands in Figure 2(C) are oblique to the rock layering. Where micro-burrow bands are exposed in large planar outcrops, they can be seen to decrease in height laterally and end into simple fractures or joints in the host rock.

Figure 3(A) shows a branched micro-burrow band, where a thin band is branching off at an angle from a broader band, with all micro-burrows positioned in the same orientation. The shorter micro-burrows along the lower branch fade into a fracture. Where blocks of marble have detached from the main outcrop, we have observed that fractures that show no evidence of micro-burrow bands on the outside of the block, may nevertheless contain micro-burrows on the broken inside surface, up to at least 20 cm from the surface of the rock. This and similar observations (Figure 3B,C) suggest that the micro-burrow bands originated along fractures inside the rock mass, even when they are now visible on the surface.

Although the micro-burrows are tightly aligned in most examples, their density does vary from outcrop to outcrop. In Figure 3(B), a surface-exposed upper micro-burrow band is now weathered, but a second band with less densely distributed micro-burrows is branching off it, with remnants of a thin white band at its upper edge. A third thin white band with even lesser developed micro-burrows is also present. In the loose specimen of Figure 3(C), calcrete separates original rock fragments containing micro-burrows. Figure 3(D) shows an outcrop *in situ*, demonstrating that the calcrete lies on top of the micro-burrows. More examples of micro-burrow bands combined with calcrete are shown in Figure S2.

The micro-burrow bands are obviously the result of replacement and removal of rock material. They differ from deposits caused by endostromatolites, which are also present in the investigated area (Figure 4A). Endostromatolites build rock material that no longer resembles the original rock, so the rock layering is not conserved (Clark et al. 2004), and the built-up material does not contain regular micro-burrows that span the complete width of a layer. Instead, their deposits contain columnar structures with macroscopically visible growth layers (Figure 4A, inset). The specimen shown in Figure 4(B) contains micro-burrows at the top and a layer of endostromatolite at the bottom.

In situ, the orientation of the micro-burrows is mostly vertical with, when present, a thin white band at the straight (upper) edge. Figure 4(C) shows a rare example of an incipient micro-burrow band above a white layer, from which well-developed micro-burrows run downwards. When micro-burrows grow upwards, they are much shorter and less well developed.

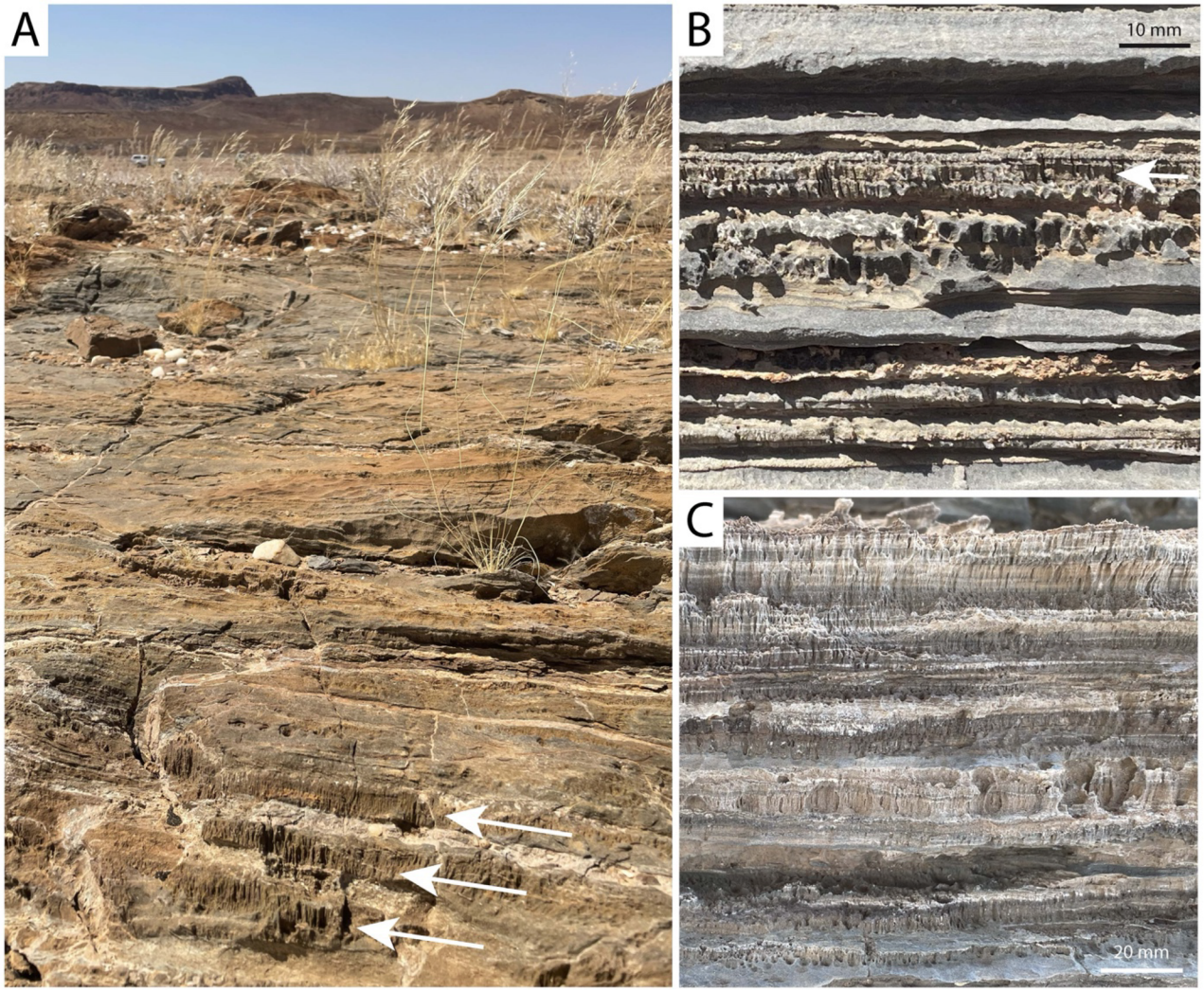

Figure 1. Field observations from Namibia. (A) Namibian desert landscape. In the foreground are three layers of marble in which micro-burrow bands are visible (white arrows). (B) Example of a single micro-burrow band (white arrow) that is clearly distinguishable from irregular karst weathering directly below it. (C) Multiple micro-burrow bands in an outcrop with various degrees of weathering. The layering in the rock is still visible in the micro-burrow bands.

Where the rock layering is folded as a result of tectonic processes, the micro-burrow bands do not follow those folds but cut through the inclined layering (Figure 4D), proving they were formed after the tectonic activity. Micro-burrows are never observed to penetrate calcrete, so we conclude the latter is formed later, still. Calcrete deposits have relatively coarse structures (Figure 3C) or lack structural features, and contain large clastic grains (Figure 3D).

When one edge of the micro-burrows is surface-exposed, their third dimension becomes visible. Figure 5(A) shows a loose specimen with narrow micro-burrows that on the surface appear as pores (Figure 5B), more clearly visible in the zooms. The pores are evenly distributed, without any visible patterns. Similar pores are observed *in situ* (Figure 5C), and when weathered, this produces a strongly solution-pitted karst surface (Figure 5D; Smith et al. 2000). The *in situ* block in Figure 5(E) contains a heavily weathered and pitted surface of eroded micro-burrows, partly covered by calcrete. Below it, a second micro-burrow band is also covered with calcrete. Once an edge of micro-burrows is surface-exposed, it increases weathering of the rock, as the pits vastly increase the exposed surface. Large-scale karst-weathering of marble outcrops resulting from the presence of micro-burrows is illustrated in Figure S3.

Micro-burrow bands similar to those found in Namibia were also observed in Oman, where they are present in layered, impure metamorphic limestones of Cretaceous age (Grobe et al. 2019), exposed on the southern flank of Jebel Akhdar anticline. The micro-burrows usually developed conformal to the layering, but are also found along vertical fractures. The micro-burrows observed in Oman are often less well developed and more widely and irregularly spaced and can be up to 50 mm long (Figure 6A). They commonly start from a white layer (Figure 6B,C). Endostromatolites are common in this area and in Figure 6(D), endostromatolites are attached to a rock also containing micro-burrow bands. Very similar structures were also seen in Neoproterozoic banded black and white marble in the Arabian-Nubian shield of Saudi Arabia (Figure 6E,F). As in Namibia, these micro-burrows branch downwards off fractures in the rock. All micro-burrow bands found in Saudi Arabia were located in black marble, and none in white marble layers in the

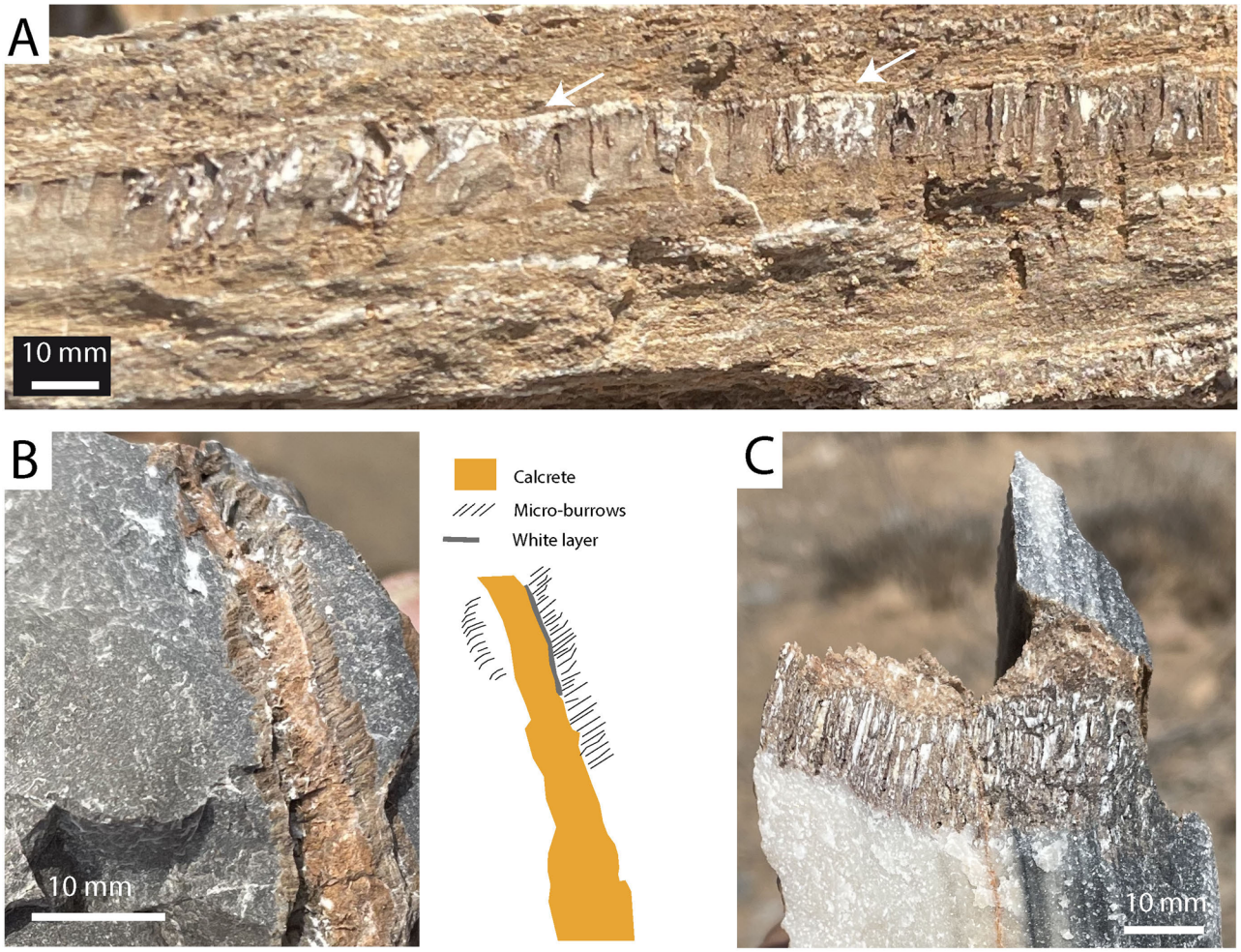

Figure 2. Micro-burrow bands - macroscopic appearance. (A) Micro-burrows are commonly filled with white material and are separated from the original rock by a sharp, straight border (white arrows). (B) The micro-burrows are frequently bordered by calcrete, often with a thin white layer in between. (C) Where layering is inclined, the micro-burrows can be nearly parallel to the rock layering; remnants of calcrete are present above the micro-burrows. B and C are loose specimens.

same outcrops. As in Oman, the micro-burrows found in Saudi Arabia are generally wider and less regular than those observed in Namibia.

Microscopy observations

In polished thin sections investigated under plain- and cross-polarized light, the marble from Namibia mainly consists of coarse calcite crystals of up to 0.2 mm in diameter, with minor traces of mica and opaque minerals (Figure 7). The micro-burrows truncate calcite crystals without clear changes in microstructure. Freshly cut rocks frequently display a discolored zone around the micro-burrows, as shown for two examples from Namibia (Figure 7). These discolored areas are also devoid of distinct changes in the crystal structure of the rock.

Micro-burrows in standard thin sections of 30 µm thickness were mostly empty, partly caused by the polishing procedure (Figure 7B–D). Thin sections of 100 µm thickness were more informative, especially when investigated with alternating transmitted and reflected light settings (Figure 7F–M). Under transmitted light, a micritic calcite filling is visible inside micro-burrows, which appears as a grey mass, and at higher magnification internal structures are visible, especially when a thin section was cut normal to the direction of the micro-burrows (Figure 7L). Commonly, this material is detached from the micro-burrow wall. In reflected light, the calcite filling of the burrows is white, in contrast to the darker colored marble host rock. When a white band is present at the top of a micro-burrow band, the white filling of the burrows grades into this white band, suggesting that the band formed from the content of the micro-burrows.

Geochemical observations

Line measurements by LA-ICP-MS were used to determine whether the composition of the white micro-burrow fillings and their associated white thin band differed from the host marble, for samples from Namibia. Metal concentrations were locally increased in the rock close to micro-burrows, but the signals were quite variable, as the composition of the marbles varied from outcrop to outcrop, and even within a sample. More consistently, the white filling of the micro-burrows and the associated white band has a lower concentration of a number of trace elements compared to the host marble (Figure S4). In particular, Sr, Mn, Fe and a number of Rare

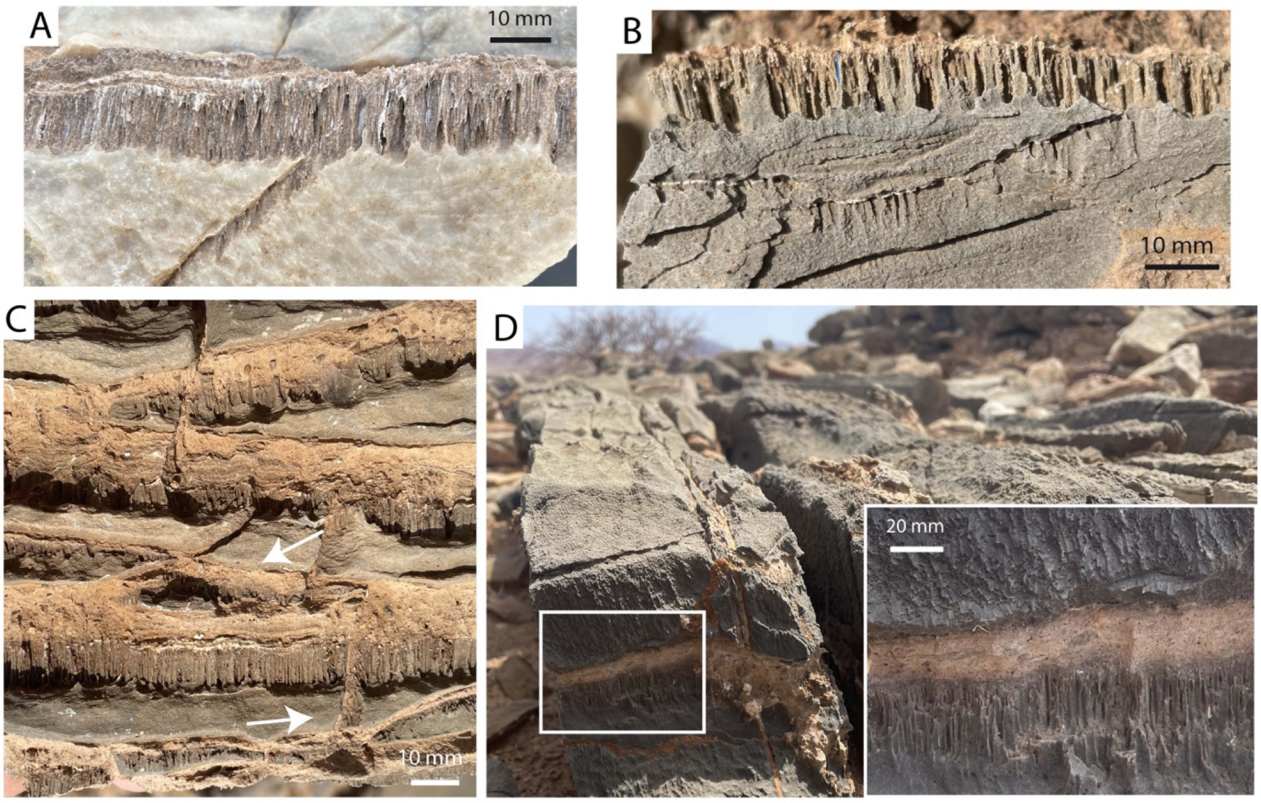

Figure 3. Link of micro-burrow bands to fractures and calcrete. (A) Branched micro-burrow band with micro-burrows having the same orientation in both branches. The lower branch ends in a fracture. (B) Three bands, the main one (top) heavily weathered as it is surface-exposed. A thin white layer is visible above the second and third band, whose density of micro-burrows is lower than that of the main band. (C) In this loose specimen, calcrete separates original rock fragments as it was formed in fractures without micro-burrows (as indicated by the white arrows) and in fractures where micro-burrows were present. In the upper part of the photo calcrete separated what originally seems to have been a Y-shaped micro-burrow band. Remnants of a white band separating the calcrete from micro-burrows are visible in the lowest micro-burrow band. (D) *In situ*, the calcrete lies on top of the micro-burrows. A close-up of the white square is shown in the zoom inset.

Earth elements (Nd, Th, Ce, Pr, and La) are present at lower abundance in the white filling (Figure S5).

EMPA was applied to produce maps of normal cut, filled micro-burrows. Elemental maps were produced for Ca, Mg, Si, P, S, Al, K, Fe, Mn, and Cl (Figure S6). Of these, Ca, K, Fe, Mn and Cl did not reveal variation, but the other elements produced complex patterns (Figure 8). The electron micrographs (last panel of each series) shows that the white filling is very fine crystalline (micritic) calcite and Mg-calcite, with delicate internal structures, that are also visible in the distribution of Mg and, in one case (Figure 8B), by Al. The rim of each filling is enriched in P and S, and at some locations in Mg and Si. P and S create contours of the micro-burrow fillings, as the white carbonate inside the micro-burrows is mostly depleted of these elements. Some of the micro-burrow rims contain structures that resemble growth rings (Figure 8D). An electron micrograph zoom is shown in Figure 8(E). The phases of these rings are approximately 1 µm wide. P and S are abundant elements of nucleic acids and proteins, respectively. The other main elements of biomolecules, C and O, would not result in useful EPMA signals due to their abundance in calcite, while N could not be determined. Likewise, Ca signals were not informative, as this was used as an internal standard. The scale of local concentration differences seen in Figure 8 explains why LA-ICP-MS, though more sensitive than EMPA, did not reveal these, as the measured LA-ICP-MS sampling spots were 50 to 100 µm wide, averaging highly localized concentration peaks.

Fluorescence microscopy

Fluorescence microscopy of the micro-burrows and their filling revealed that fluorescence in the micro-burrows was strongest at the border of the white fillings, which itself was poorly fluorescing (Figure 9). A conical cut through one of the micro-burrows revealed its three-dimensional features (Figure 9E,F).

Raman analysis

We analyzed a thin section using Micro-Raman spectroscopy (Figure 10). Here, we chose an area of interest that showed a darker material lining the inner wall of a micro-burrow (Figure 10A). Raman acquisition was complicated by the intense autofluorescence of the sample. Even after 3 minutes of fluorescence bleaching, an intense fluorescence background is visible in the raw spectra of the lining material (Figure S7A).

Three main Raman factors corresponding to the individual components could be identified by multivariate analysis: The spectral signature of calcite with characteristic band positions at 1087 (ν_1), 713(ν_4), 283 and 156 cm^{-1} (Figure 10C, green) is the main component of the micro-burrow

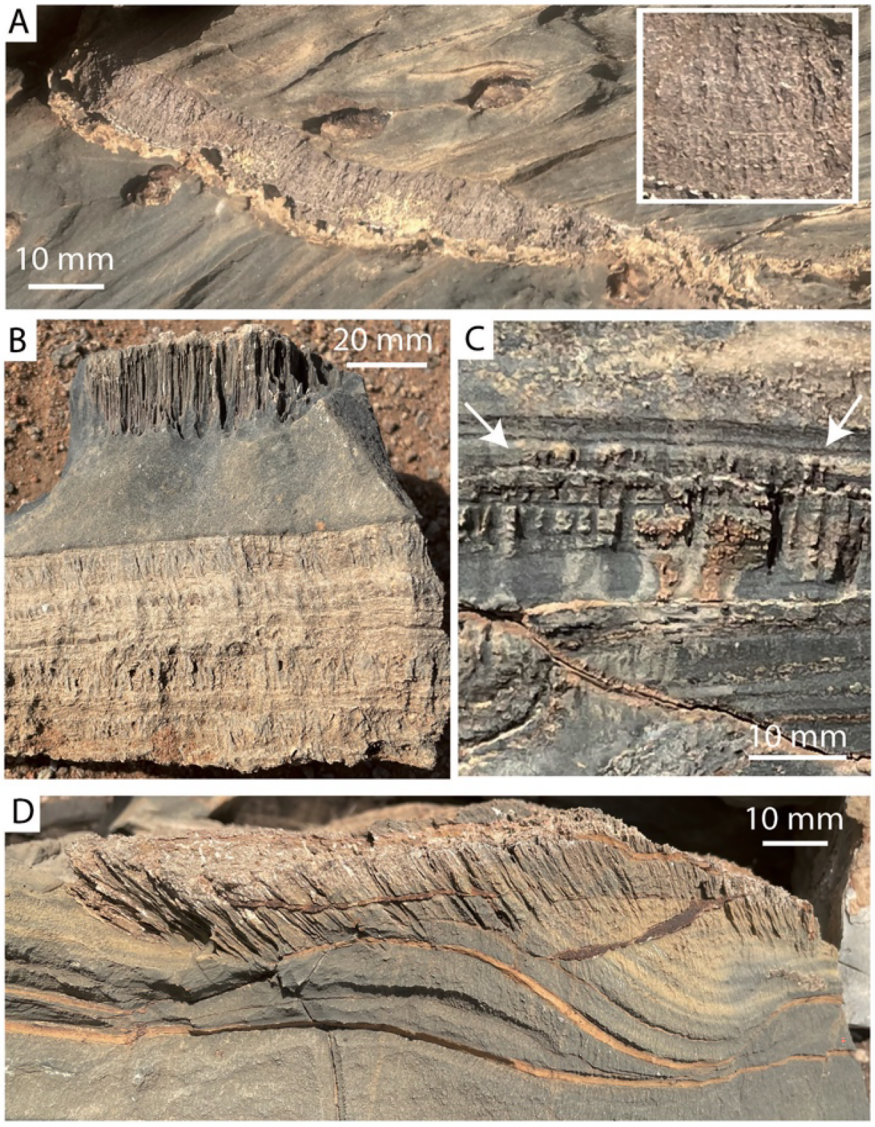

Figure 4. Micro-burrow bands and endostromatolites. (A) Endostromatolites that fill fractures result in deposits that no longer resemble the original rock and do not contain micro-burrows that extend to the complete width of a band. Inset: zoom showing the columnar structure with macroscopic growth layers that are typical for endostromatolites. (B) Loose specimen containing micro-burrows at the shown top and an endostromatolite deposit at the bottom. (C) In this heavily weathered outcrop, minor micro-burrows (indicated by arrows) formed above a thin white layer, from which the main micro-burrows developed downwards. (D) Micro-burrows formed in a folded outcrop, where they maintain their orientation despite the fold. Part of the micro-burrows are intersected by a fracture.

filling material (Figure 10B, green). Furthermore, the empty micro-burrow is filled with the embedding resin (Figure 10B, blue, for spectrum see Figure S7). In addition, carbonaceous material (CM) could be identified by the appearance of two additional broad bands at 1602 $cm^{-1}$and at 1350 cm^{-1} (Figure 10C, orange). The CM is distributed non-homogeneously with higher intensities closer to the edge and in some isolated spots (Figure 10B, orange).

Stable isotope analysis

Two samples from Namibia were used for stable isotope analysis. Both revealed a significant difference in stable isotope composition between the white and blue layering of the native rock: the blue layering produced consistently lower $\delta^{13}C$ and $\delta^{18}O$ values within a sample. Grey marble, which was close to and affected by the microburrows, had an isotope composition close to that of white marble in sample Na-2, and in between both values for sample Na-N (Figure 11). Significantly, both calcrete and the white filling of the micro-burrows produced a very different stable isotope composition from that of the host marbles, with significantly higher $\delta^{13}C$ and lower $\delta^{18}O$ values. The values obtained for the white micrite filling and for calcrete were highly similar, for both samples (Figure 11).

Discussion

The micro-burrow bands described here are quite common in marble and limestone outcrops in the deserts of Namibia and the Arabian Peninsula, although they have, to the best of our knowledge, never been described. The bands are associated with fractures in the host rock which may lie parallel to layering, but may also cut layering obliquely, branch,

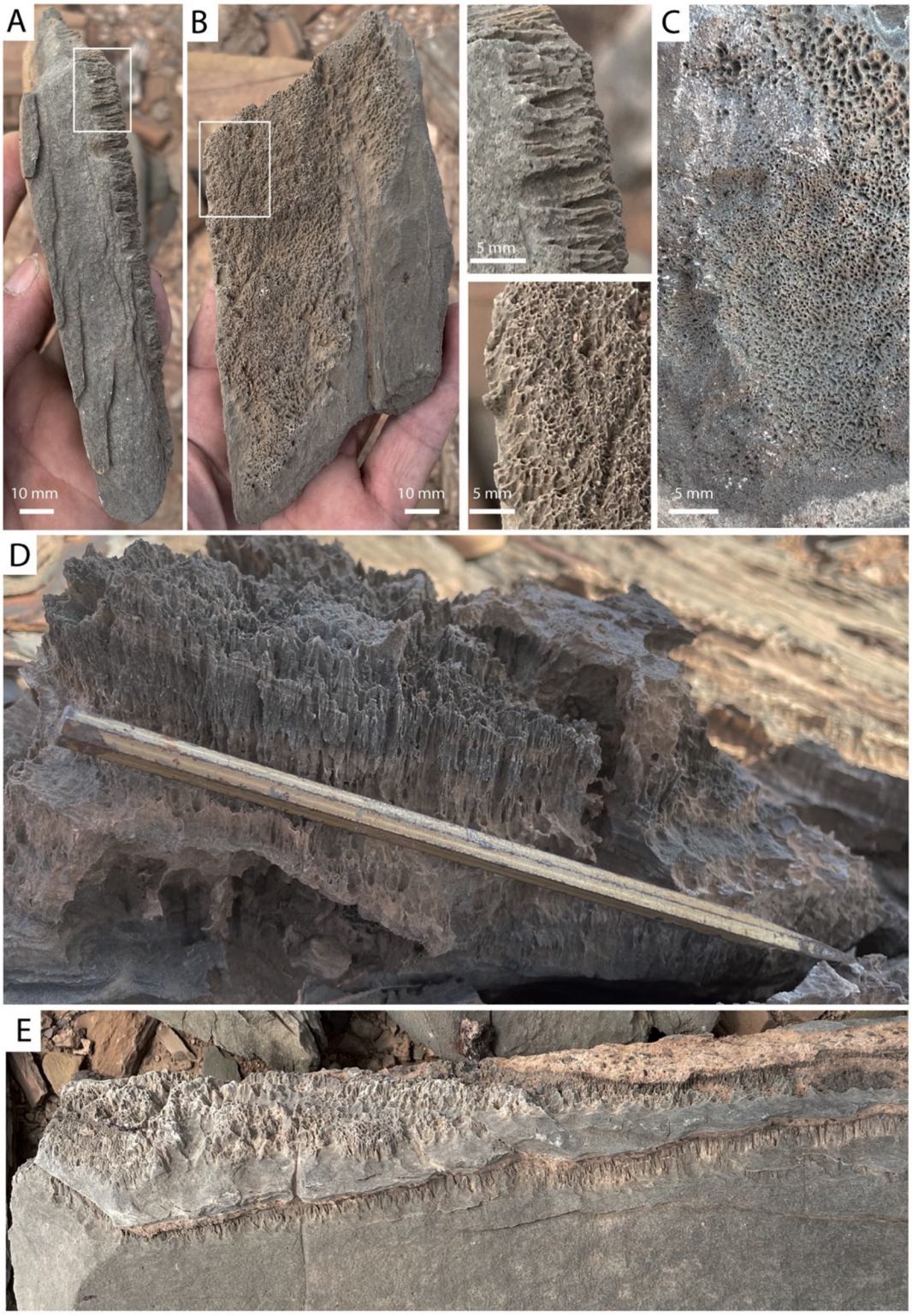

Figure 5. Micro-burrows contribute to carbonate weathering. (A, B) Loose specimen with a narrow micro-burrow band shown from the side (A) and on the surface (B), where pores are visible. The two white squares are shown as zooms to the right of B. (C) *In situ* surface showing a similar porous structure. (D) When weathered, the micro-burrows result a strongly pockmarked surface. Chisel length: 20 cm. (E) *In situ* outcrop with weathered micro-burrows, still partly covered with calcrete on its top on the right, with below it a second micro-burrow band that is still inside the rock and is also covered by calcrete.

or cut tectonic folds in marble. The micro-burrow bands are usually bound by these fractures at their top surface, which we call the basal end of the micro-burrow, while the apical end penetrates the host rock to reach various end-points inside the rock, often with a ragged edge.

Observations presented here suggest that the host rock was locally removed to create the parallel micro-burrows, whose length, diameter and morphology vary. Although the micro-burrow bands are currently mostly observed at the rock surface, they originated inside the rock and have only

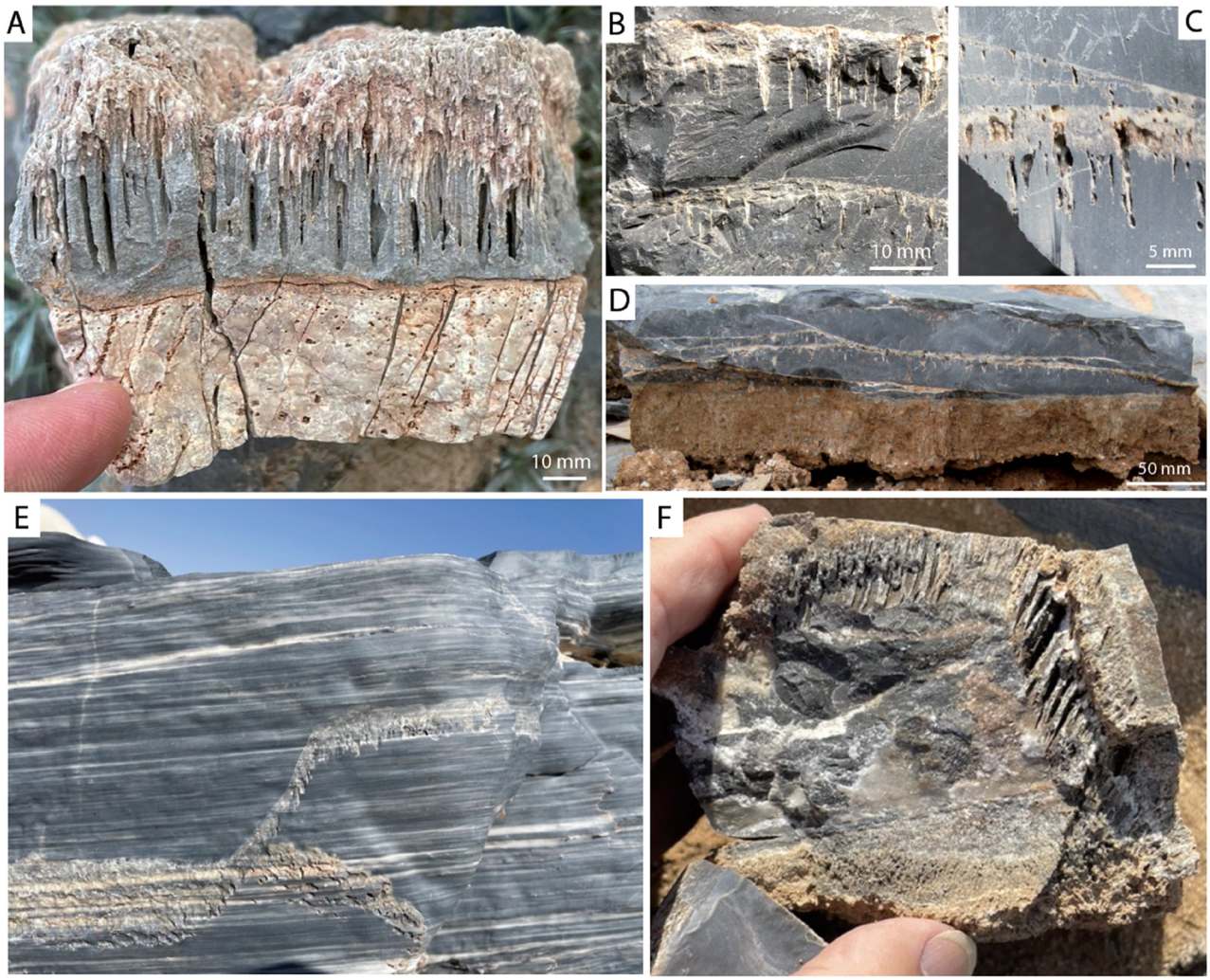

Figure 6. Examples of micro-burrows from Oman and Saudi Arabia. (A) Loose specimen with high-density micro-burrows (top half) that are partly filled with white deposit. (B) Two *in situ* bands of low-density micro-burrows filled with white material that starts from a white layer. (C) Freshly cut surface showing one well-developed and two less developed, low-density micro-burrow bands starting from a white layer. (D) Loose fragment with branched, low-density micro-burrow bands. Its bottom side is covered with a layer of endostromatolites. (A-D) from Oman. (E, F) micro-burrow bands along fractures in black marble, Saudi Arabia. F shows two micro-burrow bands of different orientations, but with parallel micro-burrows in a freshly cut sample.

been exposed by erosion. The micro-burrows formed after the metamorphic limestones were uplifted to the surface, as these fragile porous structures transect calcite crystals. As no known chemical or physical weathering mechanism can explain this phenomenon with the microstructural and geochemical observations presented here, and the micro-burrows form inside the host rock, we suggest that they are of biological origin.

The microfabric and geochemical composition of the white bands of micrite often associated with the micro-burrow bands, as well as their micrite filling that contains concentric internal structures and is detached from the rock wall, excludes their origin as abiotic vein filling. Vein calcite is coarser crystalline, would fill the entire space, and lacks the finely laminated internal structure that we observed here (Passchier and Trouw 2005).

A typical weathering pattern of limestone in which biological activity is involved is surface pitting (Gleason et al. 2017; Gorbushina 2007), which is very different from what we present here. Carbonate weathering in an arid region of Tunisia that may have been formed by biological activity (Smith et al. 2000) also does not resemble our observations. A publication describing endolithic systems in East Antarctica included field photographs (Mergelov et al. 2018), but those presented features were also different from our findings. We have observed endostromatolite deposits, both in Namibia and, far more common, in Oman (Figures 4 and 6), but those are clearly different from micro-burrow bands that were formed by removal, not by deposition of material as is the case for endostromatolites. Bungartz and Wirth (2007) describe a lichen in Namibia that produces white micrite substrate similar to the filling of our burrows. However, these organisms only form micropits on the surface of pebbles (Bungartz and Wirth 2007). Other organisms that bore into rocks such as fungi, red and green algae have also been observed in euendolithic habitats in deserts (Bungartz and Wirth 2007; Cockell and Herrera 2008; Gorbushina 2007; Wierzchos et al. 2012). Fungi secrete digestive agents, including acids, from their hyphae (Garcia-Pichel 2006). Indeed, euendolithic growth of the thalli of lichen and fungi have

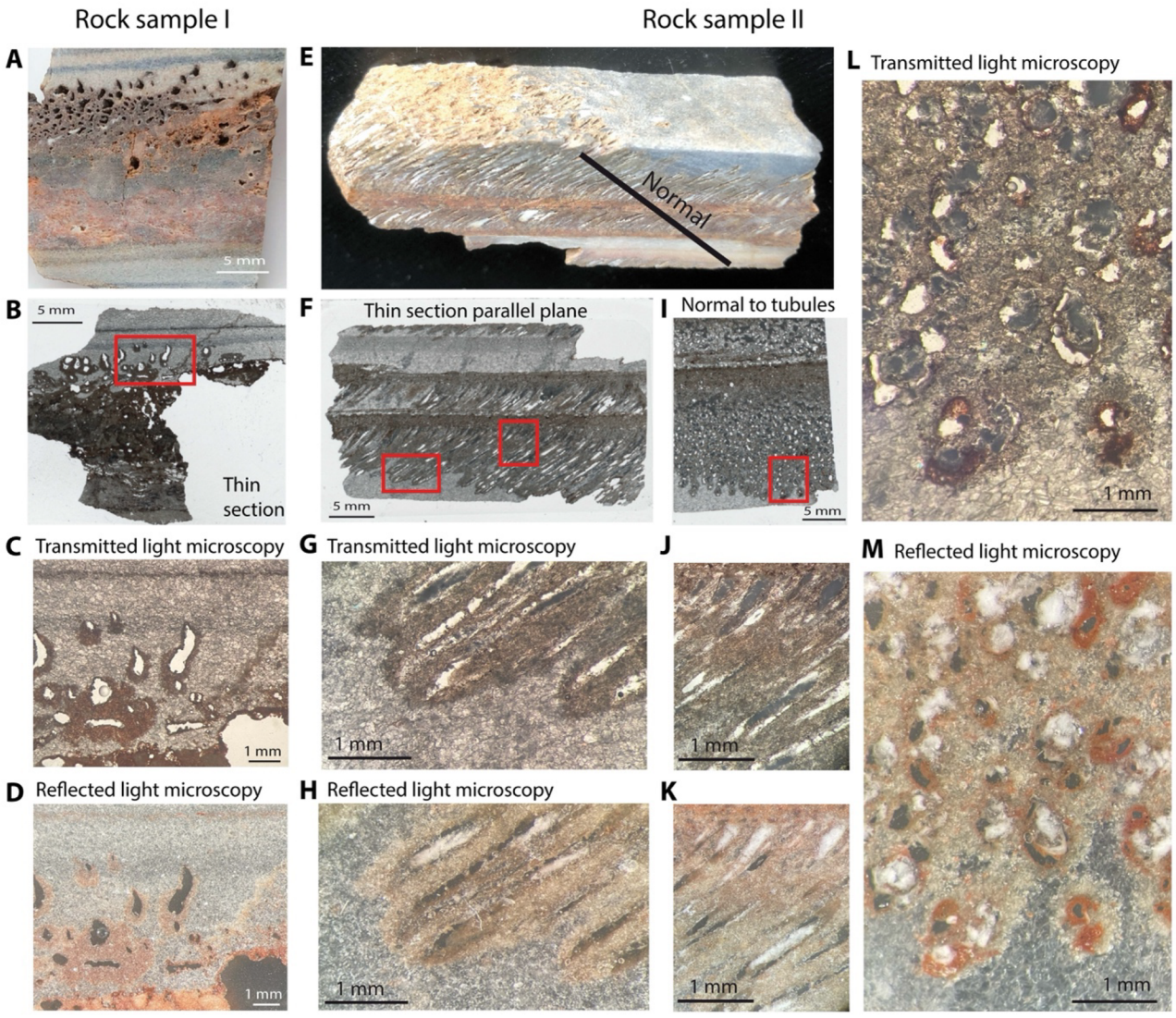

Figure 7. Microscopic observations for two typical samples from Namibia. Freshly cut surfaces often show discoloring around the micro-burrows. (A) Rock sample I was cut normal to the slanting micro-burrows, giving thin section (B). The micro-burrow holes were empty in this specimen, but the discoloring around the micro-burrows was clearly visible under transmitted light (C) and reflected light (D). (E) Rock sample II was cut to give thin sections parallel (F) and normal (I) to the micro-burrows. Areas enlarged in the micrographs are shown in red. The white filling appears dark grey under transmitted light (G, J, and L), and white under reflected light (H, K, and M). Various degrees of discoloring can be seen in M, and internal structures inside the micro-burrows are visible in (L).

been observed to penetrate rocks (Bungartz and Wirth 2007); they cause both boring tubes (Garcia-Pichel 2006; Kolo et al. 2007) and leave behind a white layer of micrite, similar to what we have observed. Fungi are also known to excrete Ca-oxalate that is transformed to calcite later (Verrecchia 2000). However, the euendoliths described in the literature so far only form shallow structures that remain close to the surface (Bungartz and Wirth 2007; Verrecchia 2000). Certain photosynthetic cyanobacteria can digest carbonate and assist in the destruction of biogenic carbonates as well as coastal limestones (Schneider and Le Campion-Alsumard 1999), but the organisms that caused the micro-burrows in Namibia are unlikely to be phototrophs, since these are restricted to depths in the order of mm only (Cockell and Herrera 2008).

We considered whether the micro-burrows could have been caused by hyphae branching off from a mycelium growing in the fracures. However, when viewed from the top, the micro-burrows are not arranged in any type of pattern, other than giving an evenly spaced distribution (Figure 5). An arrangement typical of fungal hyphae forming a mycelium is not observed. The micro-burrows also never split, cross or merge, and are always strictly parallel, which is not typical for hyphae growth.

Besides the geometry and arrangement of the micro-burrows described here, geochemical and stable isotope observations also suggest a biological origin. This applies specifically to the enrichment in P and S along the edges of the burrows, and the concentric enrichment of certain elements within the white micrite filling (Figure 8). Results of stable isotope analysis (Figure 11) produced signatures strongly resembling those of biogenic endostromatolites, suggesting this micrite filling was deposited by biological activity.

A biotic origin of the observed structures supposes the presence of liquid water, without which biological growth

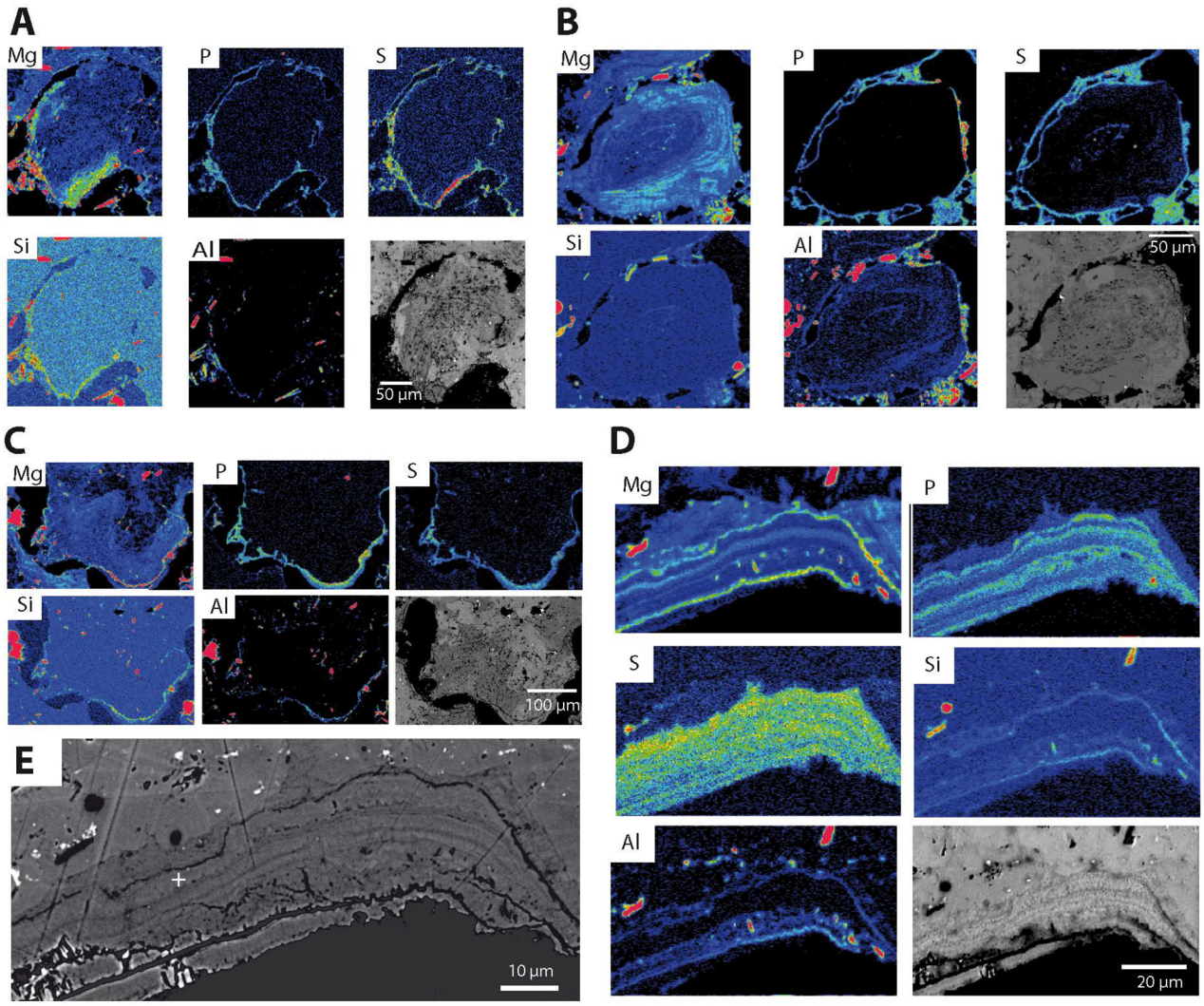

Figure 8. Electron-microprobe analysis. Four elemental maps (A–D) are shown for cross-sections of micro-burrows and their calcite filling for the five elements indicated, complemented with the electron micrograph. Blue to red show low to high concentrations. (E) Enlargement of the electron micrograph of (D), clearly shows growth rings of approximately 1 µm wide. The complete maps with color scales are presented in Figure S5.

would be impossible. The investigated areas are currently arid, but experience occasional rain showers and regular dense coastal fog, while wet periods occurred in the past, at 1–3 My in Namibia (Heine 1998; Pickford 2000) and in the Arabian Peninsula (Nicholson et al. 2020). Fractures in rock commonly carry water, and from such moist fractures the micro-burrows extend downwards into the rock, probably in response to gravitational water movement. The importance of downwards growth is supported by rare observations where micro-burrows grow upwards from a fracture, in which case they only reach a few mm in length (Figure 4C). The parallelism of micro-burrows suggests some competing mechanism. The micro-burrows are nearly always straight, but their diameter can be somewhat variable along their length and in absence of weathering, the micro-burrows become narrower toward the apical tip. The micro-burrows are much wider than the width of typical single cells of microorganisms, which would be more in the order of micrometers than the observed millimeters. This suggests a colony would have been present, which is also supported by the observed growth rings.

Bacteria have been isolated from deep rocks, where they feed on inorganic and organic material dissolved in water circulating in small fissures and fractures (Pedersen 1997), but these have not been associated with boring activity. Carbonate deposits, which are often the product of previous biological activity, can support bacterial growth. The terrestrial calcium carbonate deposits in which the micro-burrows are observed have all originated as marine sediments, before being metamorphosed into limestone or marbles. A biotic origin and the contribution of 'marine snow' would have introduced biomatter in these deposits (Macquaker et al. 2010), which in Namibia have since been exposed to high pressures and temperatures due to tectonic activity, before they were uplifted to the surface. This would have disintegrated the original biomatter to short-chain unsaturated carbohydrates or methane that might serve as a carbon and electron source for biological activity. The amount of biologically available carbon could not be assessed, as its signal is overshadowed by carbon present in the form of carbonate. SO_2 may have formed from proteins, and N may be present in small amines or amides, all of which are molecules that

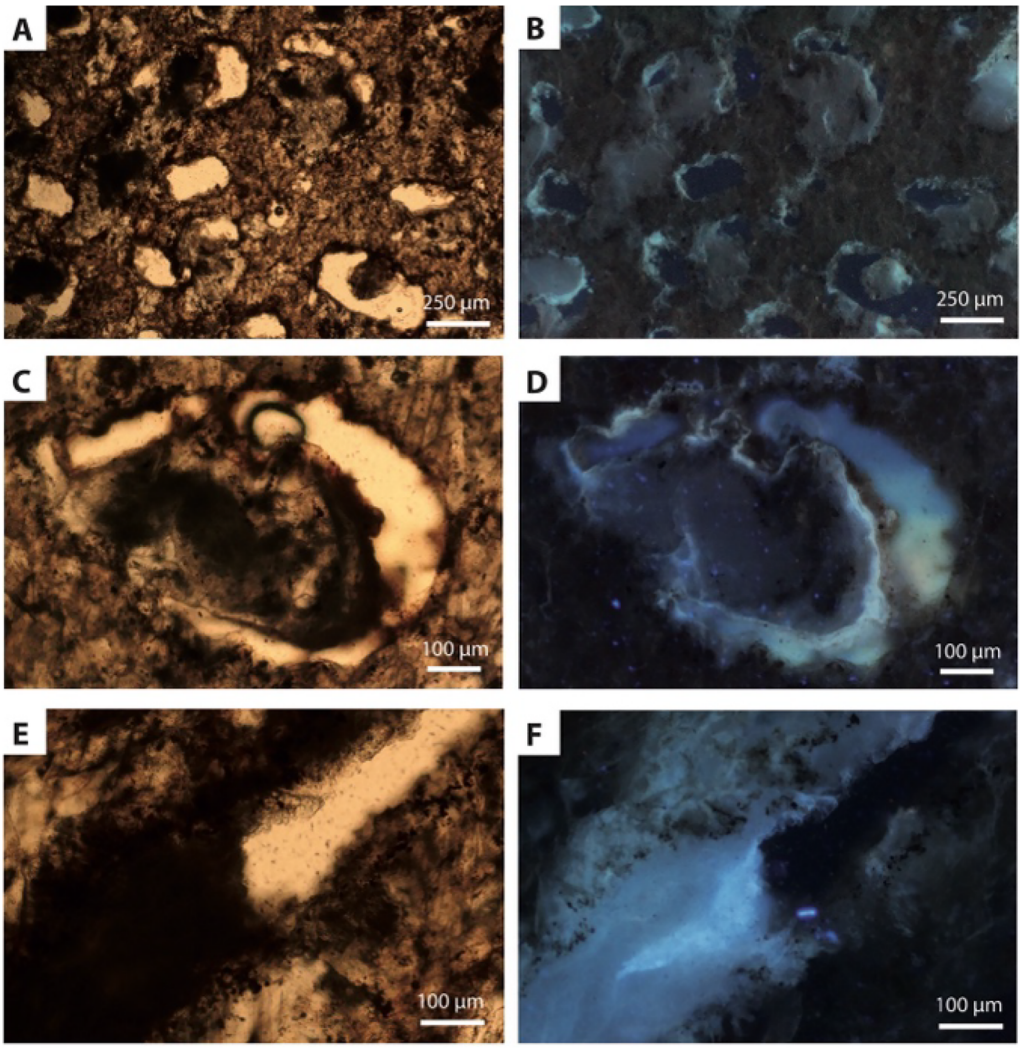

Figure 9. Fluorescence microscopy. Three examples are shown, under visible light (left) and UV (right). A-D are normal sections, E and F show a conical cut through a micro-burrow. The white filling of the micro-burrows is dark brown in visible light and dark blue under UV, except for their strongly fluorescent rims. Voids appear cream colored under visible light.

can serve as nutrients. In the Oman limestone, small amounts of hydrocarbons (bitumen) are present (Grobe et al. 2019) which may provide nutrients and energy there.

In summary, what sets the hypothetical micro-burrow producing organisms apart from currently known rock-boring organisms is (1) growth along fractures inside a rock at a depth that excludes phototrophs; (2) regular and parallel spacing of the burrows, without crossing or interconnection that would be typical for a mycelium; (3) growth in a relatively regularly spaced, three-dimensional arrangement that, viewed from the top (when exposed), lacks thread-like arrangements; (4) µm-wide growth rings present at the outer contours of the white micrite filling, suggestive of successive diametral expansion of each micro-burrow.

Based on the observations we can hypothesize a mechanism for the formation of parallel micro-burrows that lead away from the fracture from which they formed (Figure 12). Infestation of the rock would start with microorganisms entering via water that penetrate a fracture (Figure 12A). These multiply while they consume short-chain hydrocarbons and other nutrients that are captured in the carbonate and dissolved in fracture water or diffused from the surrounding rock, at the same time dissolving $CaCO_3$, possibly by secretion of acid. As the fracture environment becomes depleted of nutrients and essential elements, the community expands by growing downwards, away from the fissure. A zone of depleted nutrients and minerals eventually forms around each growing community, which not only hampers growth in any direction other than away from the fissure where competing communities are absent (further downwards), but also defines the minimal width *a* of the remaining micro-burrow wall (Figure 12A). Growth then only occurs at the apical tip of the micro-burrow, where competition for nutrients and elements ensures all colonies grow in the same direction (Figure 12B).

Material that is removed from the apical side of a beginning cavity must either be completely incorporated into biomatter, or (actively or passively) transported toward the opening at the top. This waste product, mostly micritic calcite, forms the white filling, explaining its biogenic isotope signature. Redundant calcium ions would have to be moved toward the basal end of the growing micro-burrow to create

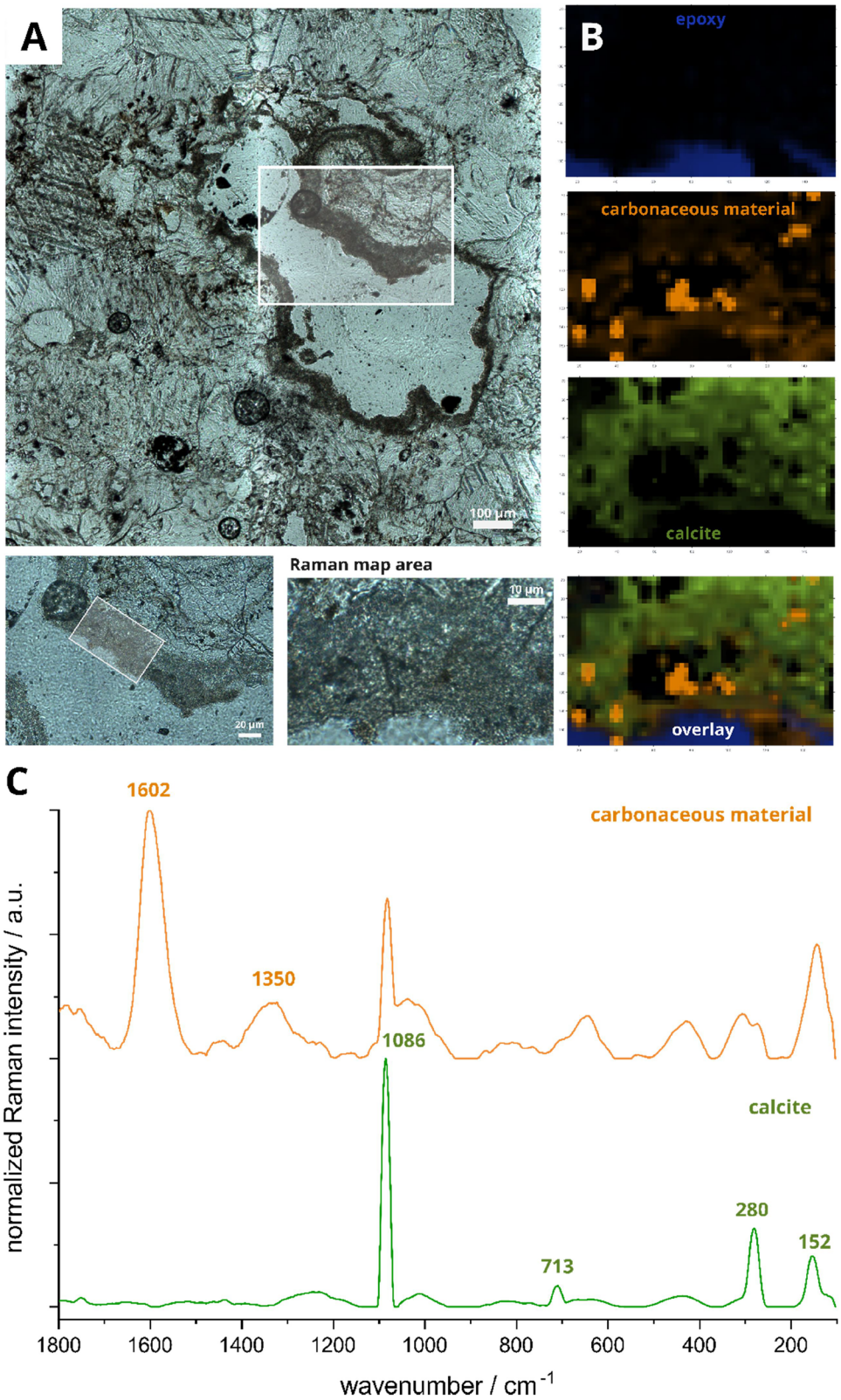

Figure 10. Raman imaging of a micro-burrow. (A) Bright field images showing several different magnifications of the region of interest, a micro-burrow with a darker lining. (B) Raman images derived by non-negative matrix factorization (NMF) showing the distribution of the individual components: the host mineral calcite (green), the embedding material (epoxy resin, blue) and carbonaceous material (orange). (C) Factors derived by NMF used for visualization in (B), showing the spectral signature of the carbonaceous material (orange) and calcite (green). All spectra are background-corrected and normalized.

the space required for growth. From there it would 'overflow' into the fracture to form the thin white layer. The movement of calcium ions can be enabled by passive diffusion, provided there is a concentration gradient along the micro-burrow, or by water, but an upwards direction of movement makes this unlikely. Alternatively, calcium ions

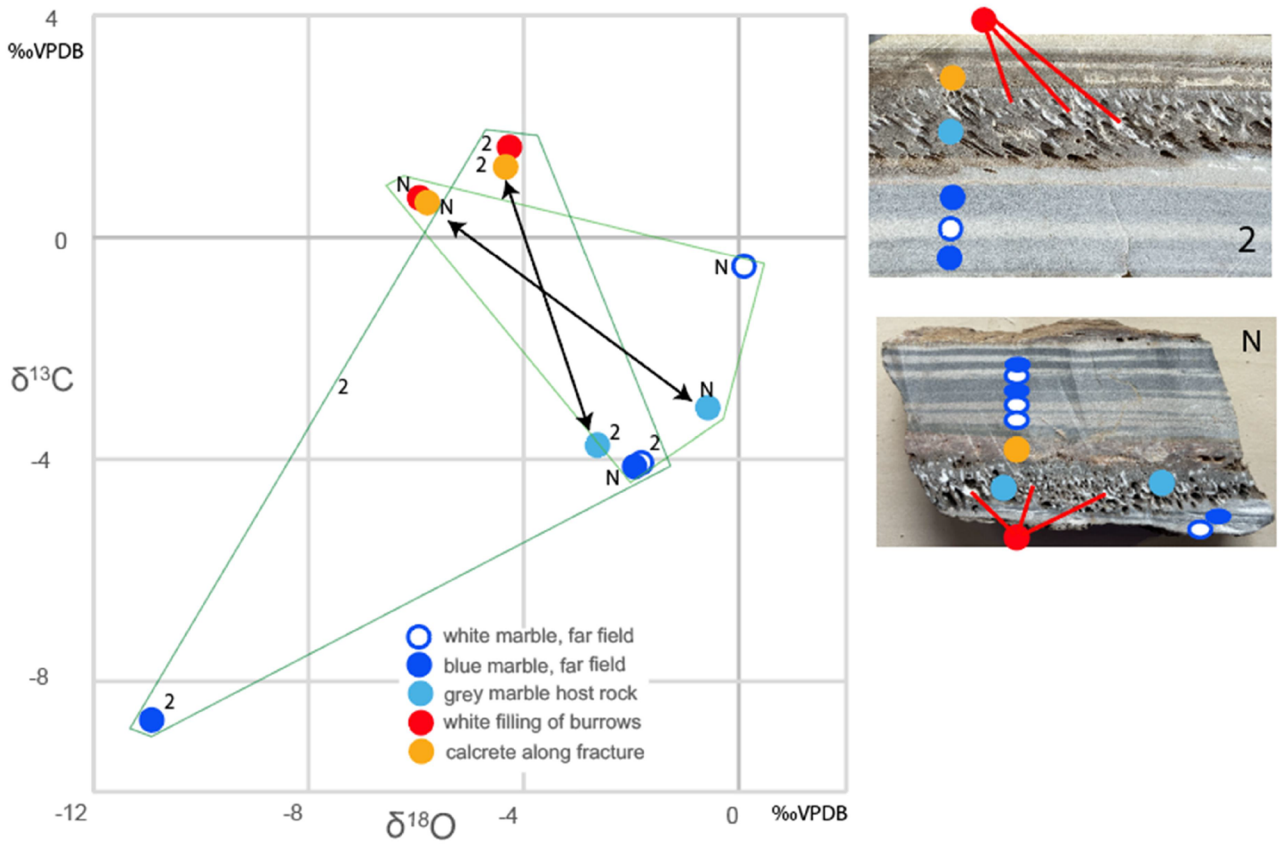

Figure 11. Stable isotope analysis of micro-burrows and host material in two samples from Namibia (NA-2, marked 2 and NA-N, marked N in panel a). Data are shown for the white micrite filling of micro-burrows (red symbols), together with that of adjacent calcrete (orange), modified grey marble (light blue symbols), and unaffected host rocks marble with blue and white layers (dark blue and white blue-rimmed symbols, respectively).

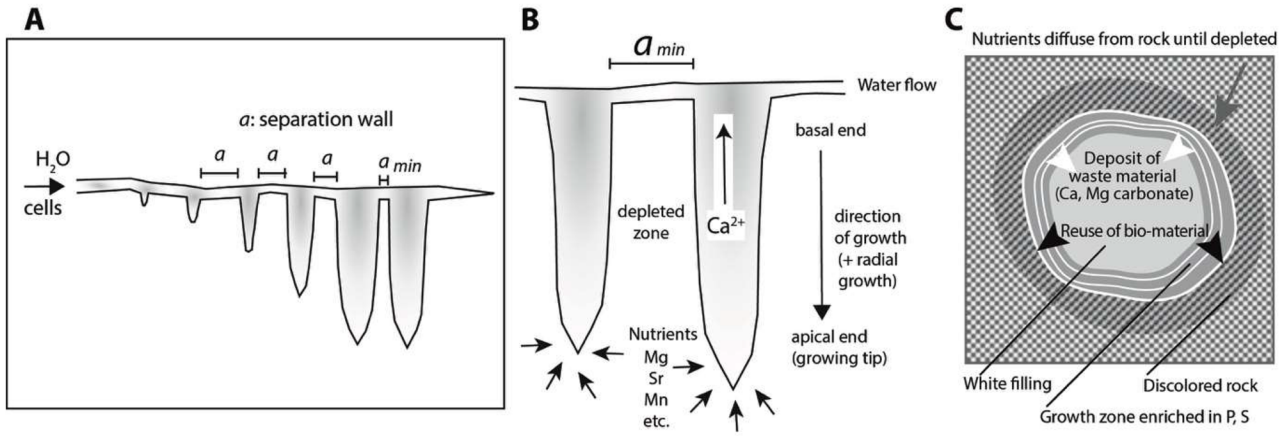

Figure 12. Schematic drawing of the proposed formation of the micro-burrows by microbes. (A) Various developmental stages toward a minimal separation a_{min} of parallel micro-burrows. (B) Zoom showing the direction of growth and movement of nutrients from the rock, for two micro-burrows. Calcium carbonate is deposited in the direction opposite of the growth direction. (C) Cross section showing how growth takes place at the rim of a micro-burrow in a radial direction, while a deposit of waste (mostly calcium minerals) is formed at the centre of the micro-burrow. The discoloring of the surrounding rock may be caused by material diffusing out of the micro-burrow during decay.

may have been actively transported from cell to cell along the micro-burrow, starting from cells accumulating it at the apical side that pass it on toward cells located more basally. Living organisms contain specific calcium pumps in their membranes, and for cyanobacteria that form micro-cavities in shells, it has been suggested these calcium pumps can be used to create low calcium concentrations at the end of their cavity, to allow diffusion (Garcia-Pichel 2006). If this also occurred in the hypothesized microbes forming the micro-burrows described here, a higher order of organization would be necessary to ensure Ca transport happens in the correct (longitudinal) direction toward the base. Such transport may pose a maximum length of any cavity that can be formed, which according to our observations is about

30 mm. Ultimately, calcium carbonate is secreted behind the growth phase where it forms a deposit. Such calcium mineral deposits have been described for *Dictyostelium*, which are multicellular eukaryotic microorganisms, when grown on calcite (Eder et al. 2016).

In addition to growth in the longitudinal direction, radial growth would increase the width of each burrow, creating growth rings, up to the maximum width that is defined by depletion of nutrients in the surrounding rock (Figure 12C). This would require Ca transport toward the center of the cavity, where over time a column of micritic calcite is formed as waste material, filling the micro-burrow. Fluorescence was found strongest at the outer edge of the white calcite filling, and both P and S are enriched there, which is where growth would take place. Once a community is present, it can maintain growth by consumption of diffusing nutrients and of dead cells, until nutrients (and energy) become limited. When eventually the biological material decays, diffusion of degraded material into the surrounding rock may be responsible for the observed discoloring.

The process as suggested above is further supported by Raman analysis. Carbonaceous material (CM) was identified by Micro-Raman spectroscopy. The characteristic first-order Raman band at 1602 cm^{-1} can be assigned to a combination of the G + D2-band (Beyssac et al. 2002). The other band at 1350 cm^{-1} corresponds to the D1-band of CM and is an indication of structural disorder and the presence of crystal defects (Kouketsu et al. 2014).

The presence of CM is attributed to the presence of organic material in metamorphic and metasedimentary rocks. Metamorphic transformation or fossilization leads to a solid-state transformation of this organic matter into a graphitic material. In conclusion, the presence of CM in the filling of the micro-burrows is a clear indication of organic matter originally deposited in the host sedimentary rock and supports a biogenic nature of the micro-burrows.

The cavities formed by the burrowing organisms proposed to be responsible for the observations presented here are now contributing to weathering. If these organisms were active on a global scale in the more recent past, this would have had strong implications on the global carbon cycle in those periods, and they may still affect present rates of erosion and weathering. Their contribution toward global carbon cycles deserves further studies. If this limestone-consuming and erosion-enhancing biological activity has taken place on a large enough scale, its contribution to the global carbon cycles would need to be incorporated in models to accurately describe past processes. Whether this would affect predictions about future carbon cycling remains to be seen.

We can presently only speculate about the possible organisms responsible for the formation of micro-burrow bands. This paper serves to describe our observations in the hope that similar features have been observed and identified elsewhere. Further attempts can be made to identify the responsible organisms, but the subfossil nature of the micro-burrows makes it unlikely that DNA survives. Although most biological macromolecules will have disintegrated over time because of the considerable age of the micro-burrows (estimated at more than 1 Ma) and the strong weathering in desert conditions, the elements from which they were made up are still locally detectable and degraded biological material still results in fluorescence.

Acknowledgment

We thank Corinna R. Schott for preliminary investigations performed during her undergraduate study.
We thank Prof. Christoph Spötl, University of Innsbruck, for stable isotope analyses of two samples. We thank Prof. Mahrous Abu El-Enen for guidance in the field in Saudi Arabia, and the Saudi Geological Survey and the China Geological Survey for logistic support there.

Disclosure statement

The authors report there are no competing interests to declare.

Dedication

This work is dedicated to our colleague and friend Janos Urai, who was involved in collection of samples from Oman, but sadly passed away before finalization of the manuscript.

Funding

Field studies in Namibia were funded by the Schürmann Foundation, the Netherlands (CWP).

Data availability statement

The raw data from EMPA and ICPMS analyses are available from the corresponding author upon reasonable request. Rock samples are available upon request.

References

Beyssac O, Goffé B, Chopin C, Rouzaud JN. 2002. Raman spectra of carbonaceous material in metasediments: a new geothermometer. J Metamorph Geo 20(9):859–871.
Bungartz F, Wirth V. 2007. *Buellia peregrina* sp. nov., a new, euendolithic calcicolous lichen species from the Namib Desert. Lichenologist 39(1):41–45.
Clark ID, Lauriol B, Marschner M, Sabourin N, Chauret Y, Desrochers A. 2004. Endostromatolites from permafrost karst Yukon Canada: paleoclimatic proxies for the Holocene thermal hypsithermal. Can J Earth Sci 41(4):387–399.
Cockell CS, Herrera A. 2008. Why are some microorganisms boring? 2008. Trends Microbiol 16(3):101–106.
Dievart AM, McQuaid CD, Zardi GI, Nicastro KR, Froneman PW. 2022. Photoautotrophic euendoliths and their complex ecological effects in marine bioengineered ecosystems. Diversity 14(9):737.
Eder M, Koch M, Muth C, Rutz A, Weiss IM. 2016. *In vivo* modified organic matrix for testing biomineralization-related protein functions in differentiated *Dictyostelium* on calcite. J Struct Biol 196(2):85–97.
Frimmel HE, Miller RM. 2009. Continental rifting Neoproterozoic to Early Palaeozoic evolution of Southwestern Africa. In: Gaucher C, Sial AN, Halverson GP, Frimmel HE, editors. Neoproterozoic-Cambrian Tectonics Global Change and Evolution: A Focus on Southwestern Gondwana. Developments in Precambrian Geology. Vol. 16. Elsevier: Amsterdam;, p153–159.
Garcia-Pichel F. 2006. Plausible mechanisms for the boring on carbonates by microbial phototrophs. Sediment Geol 185:05–213.

Gleason FH, Gadd GM, Pitt JI, Larkum AWD. 2017. The roles of endolithic fungi in bioerosion and disease in marine ecosystems. I. General concepts. Mycology 8(3):205–215.
Golubic S, Friedmann I, Schneider J. 1981. The lithobiontic ecological niche with special reference to microorganisms. J Sediment Petrol 51:475–478.
Gorbushina AA. 2007. Life on the rocks. Environ Microbiol 9(7):1613–1631.
Grobe A, von Hagke C, Littke R, Dunkl I, Wübbeler F, Muchez P, Urai JL. 2019. Tectono-thermal evolution of Oman's Mesozoic passive continental margin under the obducting Semail Ophiolite: a case study of Jebel Akhdar Oman. Solid Earth 10(1):149–175.
Heine K. 1998. Climate change over the past 135 000 Years in the Namib Desert (Namibia) derived from proxy data. Palaeoecology of Africa and the surrounding islands. p171–198.
Jochum KP, Nohl U, Herwig K, Lammel E, Stoll B, Hofmann AW. 2005. GeoReM: a new geochemical database for reference materials and isotopic standards. Geostand Geoanalyt Res 29(3):333–338.
Jochum KP, Weis U, Stoll B, Kuzmin D, Yang Q, Raczek I, Jacob DE, Stracke A, Birbaum K, Frick DA, et al. 2011. Determination of reference values for NIST SRM 610–617 glasses following ISO guidelines. Geostandard Geoanalytic Res 35(4):397–429.
Kolo K, Keppens E, Préat A, Claeys P. 2007. Experimental observations on fungal diagenesis of carbonate substrates. J Geophys Res 112(G1):G01007.
Kouketsu Y, Mizukami T, Mori H, Endo S, Aoya M, Hara H, Nakamura D, Wallis S. 2014. A new approach to develop the Raman carbonaceous material geothermometer for low-grade metamorphism using peak width. Isl Arc 23(1):33–50.
Lacelle D, Pellerin A, Clark ID, Lauriol B, Fortin D. 2009. Micro)morphological inorganic–organic isotope geochemisty and microbial populations in endostromatolites (cf fissure calcretes) Haughton impact structure Devon Island Canada: The influence of geochemical pathways on the preservation of isotope biomarkers. Earth Planetary Sci Lett 281(3-4):202–214.
Macquaker JHS, Keller MA, Davies SJ. 2010. Algal blooms and "marine snow": Mechanisms that enhance preservation of organic carbon in ancient fine-grained sediments. J Sedimentary Res 80(11):934–942.
Mergelov N, Mueller CW, Prater I, Shorkunov I, Dolgikh A, Zazovskaya E, Shishkov V, Krupskaya V, Abrosimov K, Cherkinsky A, et al. 2018. Alteration of rocks by endolithic organisms is one of the pathways for the beginning of soils on Earth. Sci Rep. 8(1):3367.
Miller RM. 1983. The Pan-African Damara Orogen of South Africa/Namibia. In: Miller R McG, editor. Evolution of the Damara Orogen of South West Africa/Namibia, Vol. 11. Johannesburg: Geological Society of South Africa Special Publication, p431–515.
Nicholson SL, Pike AWG, Hosfield R, Roberts N, Sahy D, Woodhead J, Cheng H, Edwards RL, Affolter S, Leuenberger M, et al. 2020. Pluvial periods in Southern Arabia over the last 1 1 million-years. Quat Sci Rev 229:106112.
Passchier CW, Trouw RAJ. 2005. Microtectonics. Berlin, Heidelberg: Springer-Verlag.
Pedersen K. 1997. Microbial life in deep granitic rock. FEMS Microbiol Rev 20(3–4):399–414.
Pickford M. 2000. Neogene and quaternary vertebrate biochronology of the Sperrgebiet and Otavi Mountainland Namibia. Commun Geol Surv Namibia 12:411–419.
Porada H. 1979. The Damara-Ribeira orogen of the Pan-African/Brasiliano cycle in Namibia (South West Africa) and Brazil as interpreted in terms of continental collision. Tectonophysics 57(2-4):237–265.
Prave AR, Hoffmann KH. 1995. Unequivocal evidence for two Neoproterozoic glaciations in the Damara succession of Namibia. 27 Abstract with Program Geological Society America :380.
Prentice IC, Farquhar GD, Fasham MJR, Goulden ML, et al. 2001. Intergovernmental panel on climate change The carbon cycle and atmospheric carbon dioxide https://hal archives-ouvertes fr/hal-03333974.
Schneider J, Le Campion-Alsumard T. 1999. Construction and destruction of carbonates by marine and frewshwater cyanobacteria. Eur J Phycol 34(4):417–426.
Shaw PA, Thomas DSG. 1996. The quaternary Palaeoenvironmental history of the Kalahari Southern Africa. J Arid Environ 32(1):9–22.
Smith BJ, Warke PA, Moses CA. 2000. Limestone weathering. In: Contemporary Arid Environments: A case Study from Southern Tunisia Earth Surf Process Landforms. Vol. 25. Bognor Regis: John Wiley & Sons Ltd;p. 1343–1354.
Spötl C, Vennemann TW. 2003. Continuous-flow isotope ratio mass spectrometric analysis of carbonate minerals. Rapid Commun Mass Spectrom 17(9):1004–1006.
Tanhua T, Bates NR, Körtzinger A. 2013. The marine carbon cycle and ocean carbon inventories. Int Geophys 103:787–815.
Verrecchia E. 2000. Fungi and sediments. In: Riding, RE and Awramik SM, editors. Microbial Sediments, Berlin Heidelberg: Springer-Verlag.
Wierzchos J, Casero MC, Artieda O, Ascaso C. 2018. Endolithic microbial habitats as refuges for life in polyextreme environment of the Atacama Desert. Curr Opin Microbiol 43:124–131.
Wierzchos J, de los Ríos A, Ascaso C. 2012. Microorganisms in desert rocks: the edge of life on Earth. Int Microbiol 15:171–181.